

## Supplementary Information

### A Class of Transition Metal-oxide@MnO<sub>x</sub> Core-shell Structured Oxygen Electrocatalysts for Reversible O<sub>2</sub> reduction and Evolution Reactions

Yi Cheng<sup>a</sup>, Shuo Dou<sup>b</sup>, Martin Saunders<sup>c</sup>, Jin Zhang<sup>a</sup>, Jian Pan<sup>a</sup>, Shuangyin  
Wang<sup>b</sup>, San Ping Jiang<sup>a†</sup>

<sup>a</sup> Fuels and Energy Technology Institute & Department of Chemical Engineering, Curtin

University, Perth, WA 6102, Australia

† Correspondence - [S.Jiang@curtin.edu.au](mailto:S.Jiang@curtin.edu.au) (SP Jiang)

<sup>b</sup> State Key Laboratory of Chem/Bio-Sensing and Chemometrics, College of Chemistry and

Chemical Engineering, Hunan University, Changsha 410082, Hunan, China.

<sup>c</sup> State Key Laboratory of Chem/Bio-  
Sensing and Chemometrics  
College of Chemistry and Chemical  
Engineering, Hunan University  
Yuelushan, Changsha, Hunan, 410082  
(P.R. China)  
State Key Laboratory of Chem/Bio-  
Sensing and Chemometrics  
College of Chemistry and Chemical  
Engineering, Hunan University

Yuelushan, Changsha, Hunan, 410082  
(P.R. China)

<sup>c</sup> Centre for Microscopy, Characterization and Analysis (CMCA), The University of Western

Australia, Clawley, WA 6009, Australia

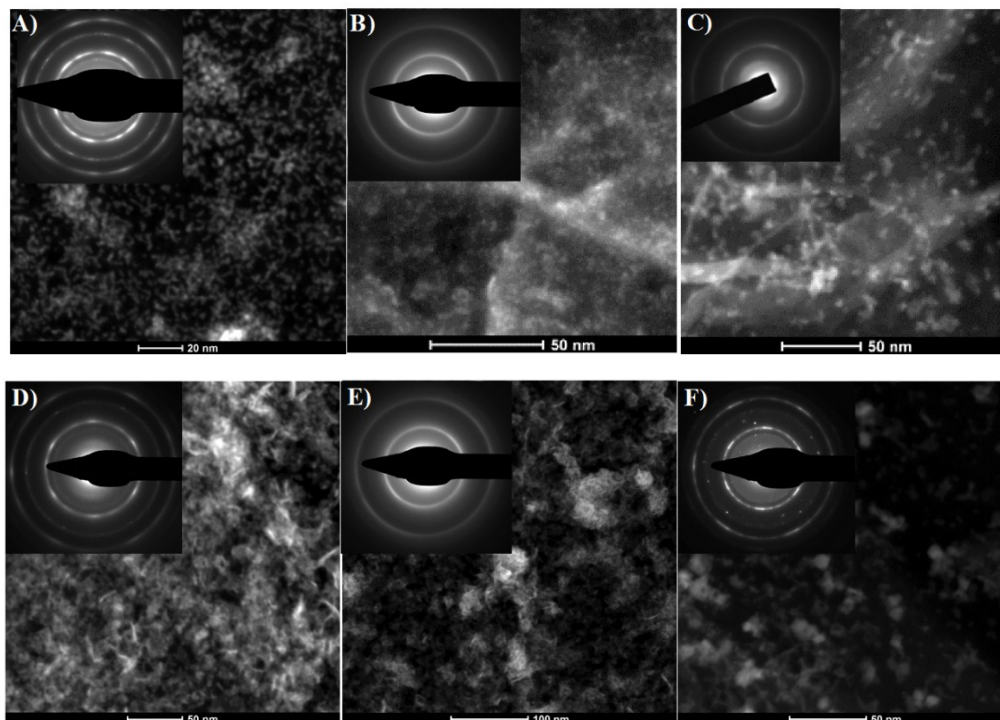


**Figure S1.** STEM images and diffraction patterns of A) NiO, B) NiFeO, C) FeO, D) NiO@MnO<sub>x</sub>, E) NiFeO@MnO<sub>x</sub> and F) FeO@MnO<sub>x</sub>.

Figure S1 show the STEM image and the diffraction patterns of NiO, NiFeO, FeO, NiO@MnO<sub>x</sub>, NiFeO@MnO<sub>x</sub> and FeO@MnO<sub>x</sub>. In the case of NiO and NiO@MnO<sub>x</sub>, four diffraction pattern were obtained which is likely attributed to  $\sim 0.24$  nm spacing,  $\sim 0.21$  nm spacing,  $\sim 0.15$  nm spacing and  $\sim 0.12$  nm spacing, which is might corresponded to the NiO(111), NiO(002), NiO(220) and NiO(113). On the other hand, the multilayer graphene mixture might also show some diffraction patterns that are corresponding to graphite(100) ( $\sim 0.21$ nm), graphite(110) ( $\sim 0.12$ nm) and graphite interlayer ( $\sim 0.34$  nm).<sup>1</sup> Hence, the diffraction pattern of NiO and NiO@MnO<sub>x</sub> is likely the overlying of the diffraction pattern from both NiO and multilayer graphene. NiFeO and NiFeO@MnO<sub>x</sub> exhibits similar diffraction patterns, the diffraction pattern is corresponding to graphite(100) ( $\sim 0.21$ nm) and graphite(110) ( $\sim 0.12$ nm),<sup>1</sup> disclosing the metal oxide are amorphous for both NiFeO and NiFeO@MnO<sub>x</sub>. For FeO, the diffraction pattern is corresponding to graphite(100) ( $\sim 0.21$ nm), graphite(110) ( $\sim 0.12$ nm), indicating that FeO is amorphous. While FeO@MnO<sub>x</sub>, except the diffraction ring for graphite(100) ( $\sim 0.21$ nm) and graphite(110) ( $\sim 0.12$ nm) that originated from the multilayer graphene, there are two

independent spot or ring that corresponding to the  $\sim 0.185$  nm spacing and  $\sim 0.267$  nm spacing is likely originated from the crystallized  $\text{Fe}_2\text{O}_3$ .<sup>2,3</sup> These results are consistent with the XRD results. However, no diffraction pattern was obtained that was origin from the  $\text{MnO}_x$ , indicating that the amorphous nature of the  $\text{MnO}_x$ .

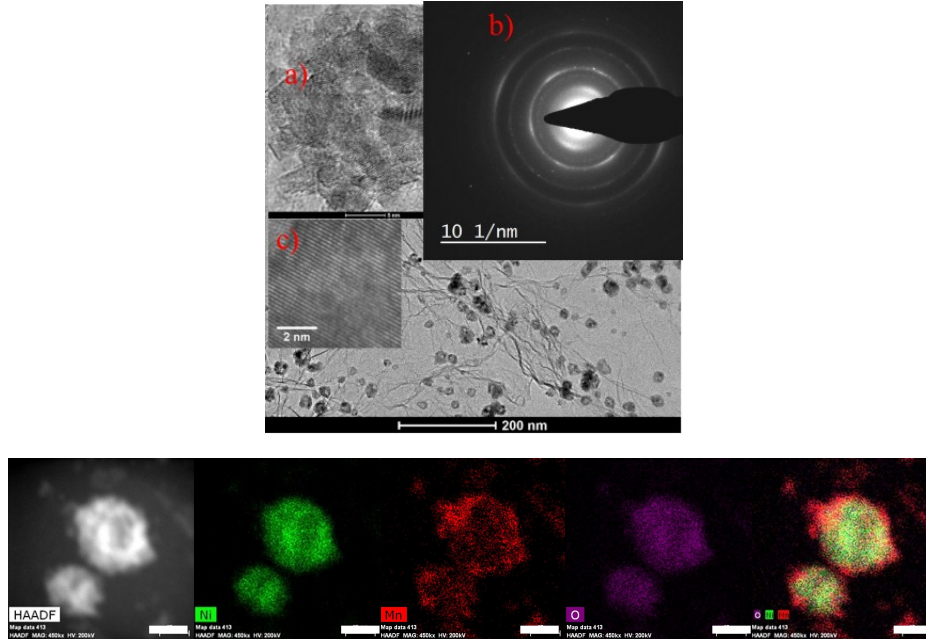


**Figure 2.** the TEM images and the STEM-EDS mapping of NiO core- $\text{MnO}_x$  shell structure synthesized using large NiO particles.

The  $\text{H}_2\text{O}_2$  yield and the electron transfer number are calculated according to the formulas:<sup>4</sup>

$$H_2O_2\% = \frac{200 \frac{I_R}{N}}{\left(\frac{I_R}{N} + I_D\right)} \quad (1)$$

$$n = \frac{4I_D}{\left(\frac{I_R}{N} + I_D\right)} \quad (2)$$

where  $I_D$  is the disk current,  $I_R$  is the ring current,  $N$  is the collection efficiency and  $n$  is the electron transfer number.

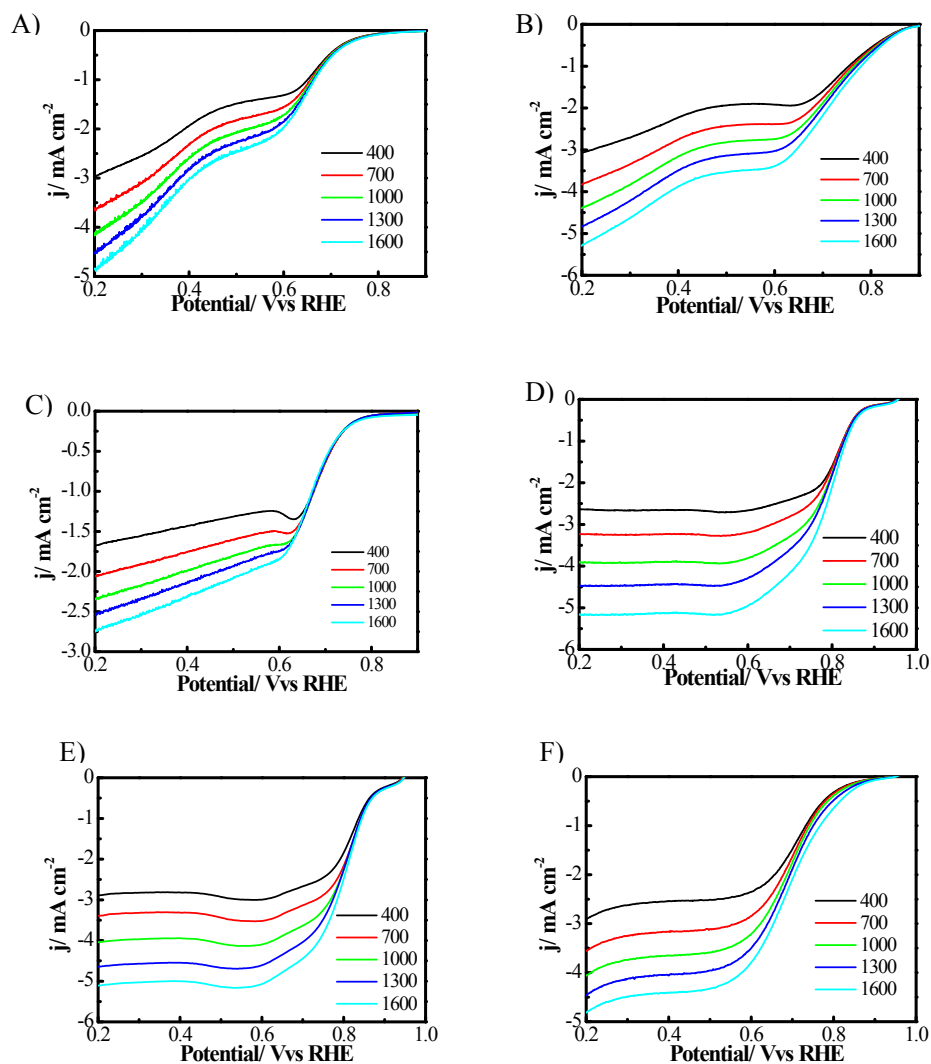


**Figure S3.** The LSV curves for ORR at different rotating speed for A) FeO, B) NiFeO, C) NiO, D) NiO@MnO<sub>x</sub>, E) NiFeO@MnO<sub>x</sub> and F) FeO@MnO<sub>x</sub> obtained in O<sub>2</sub>-saturated 0.1 M KOH at scan rate of 10 mV s<sup>-1</sup> with catalysts loading of 0.1 mg cm<sup>-2</sup>.

RDE voltammetry measurements were also carried out to gain further insight on the ORR performance of the NiO, NiFeO, FeO, NiO@MnO<sub>x</sub>, NiFeO@MnO<sub>x</sub> and FeO@MnO<sub>x</sub> electrodes. Figure S3A-F shows RDE current-potential curves at different rotation rates for various electrodes. As can be seen, the limiting current density increases with increasing rotation rate. The transferred electron number per oxygen molecule involved in the oxygen reduction at electrode was determined by the Koutechy–Levich equation given below:

$$\frac{1}{j} = \frac{1}{j_k} + \frac{1}{B\omega^{0.5}} \quad (1)$$

where  $j_k$  is the kinetic current and  $\omega$  is the electrode rotating rate.  $B$  could be determined from the slope of K-L plots based on Levich equation as follows:

$$B = 0.2nF(D_{O_2})^{2/3}\nu^{-1/6}C_{O_2} \quad (2)$$

where  $n$  represents the number of electrons transferred per oxygen molecule,  $F$  is the Faraday constant ( $F = 96485 \text{ C mol}^{-1}$ ),  $D_{O_2}$  is the diffusion coefficient of  $O_2$  in 0.1 M KOH ( $1.9 \times 10^{-5} \text{ cm}^2 \text{ s}^{-1}$ ),  $\nu$  is the kinetic viscosity ( $0.01 \text{ cm}^2 \text{ s}^{-1}$ ), and  $C_{O_2}$  is the bulk concentration of  $O_2$  ( $1.2 \times 10^{-6} \text{ mol cm}^{-3}$ ). The constant 0.2 is adopted when the rotation speed is expressed in rpm.

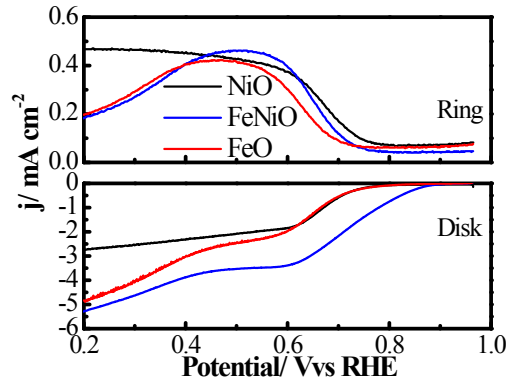


**Figure S4.** The plots of ring and disk current of ORR on NiO, NiFeO and FeO electrode measured with a rotating ring-disk electrode.

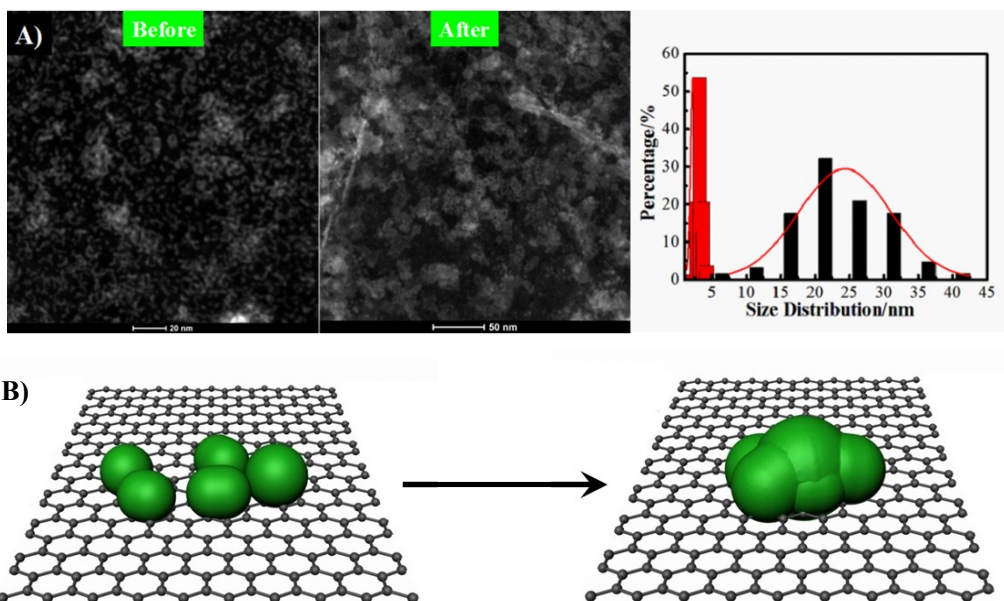


**Figure S5.** A) NiO before and after reversible OER and ORR cycling, and B) The schematic shows the aggregation of NiO nanoparticles.

### References

1. Y. Hernandez, V. Nicolosi, M. Lotya, F. M. Blighe, Z. Sun, S. De, I. T. McGovern, B. Holland, M. Byrne, Y. K. Gun'Ko, J. J. Boland, P. Niraj, G. Duesberg, S. Krishnamurthy, R. Goodhue, J. Hutchison, V. Scardaci, A. C. Ferrari and J. N. Coleman, *Nat Nano*, 2008, **3**, 563-568.
2. B. Xu, B. Huang, H. Cheng, Z. Wang, X. Qin, X. Zhang and Y. Dai, *Chem. Commun.*, 2012, **48**, 6529-6531.
3. M. Du, C. Xu, J. Sun and L. Gao, *J. Mater. Chem. A*, 2013, **1**, 7154-7158.
4. B. Aghabarari, M. V. Martinez-Huerta, M. Ghiaci, J. L. G. Fierro and M. A. Pena, *RSC Advances*, 2013, **3**, 5378-5381.